International Journal of Microwave and Wireless Technologies, 2017, 9(4), 903–913.
doi:10.1017/S1759078716000738

RESEARCH PAPER

Analysis and design of a triple band metamaterial simplified CRLH cells loaded monopole antenna

MAHMOUD ABDELRAHMAN ABDALLA[1], ZHIRUN HU[2] AND CAHYO MUVIANTO[2]

The design and analysis of meta-material inspired loaded monopole antenna for multiband operation are reported. The proposed antenna consists of multi resonators inspired from half mode composite right/left handed cells, which has a simple structure, compact size, and provides multiband functionalities. As a proof of concept, a triple band antenna covering all possible WiMAX operating bands, has been designed, fabricated, and characterized. The hosting monopole patch itself generates resonance for 3.3–3.8 GHz band, whereas the loaded metamaterial cells add extra resonance frequencies. The loading of two resonator cells introduces two extra resonances for 2.5–2.7 GHz and 5.3–5.9 GHz bands, respectively. The antenna's operating principle and design procedures with the aid of electromagnetic full wave simulation and experimental measurements are presented. The antenna has good omnidirectional patterns at all three bands. The monopole patch size is 13.5 × 6.5 mm² and the whole antenna size (including the feed line) is 35 × 32 mm². Compared with conventional single band microstrip patch radiator, the radiator size of this antenna is only 8.5% at 2.5 GHz, 17% at 3.5 GHz, and 37% at 5.5 GHz.

Keywords: Meta-material, Multiband antenna, Omnidirectional antenna, CRLH transmission line, Half- mode CRLH, WiMAX

Received 13 January 2016; Revised 30 May 2016; Accepted 1 June 2016; first published online 22 June 2016

I. INTRODUCTION

Since the early years this century, there has been a numerous increase in the wireless communication services that operate at different frequency spectrums. Also, the same wireless service (WiMAX for example) may operate at different frequency bands. One solution for multiband system is to receive the whole services using wideband antennas. However, wideband antennas generally have low received signal level, which may decrease the signal to noise ratio at the receiver terminals [1]. Therefore, the other solution is to use multiband antennas. Printed monopole antenna is attractive for wireless applications thanks to its low-cost, omnidirectional radiation pattern. Also, it can provide both broadband and multiband operations [2, 3]. It can be designed in different shapes, such as rectangular, circular and other shapes in microstrip and coplanar waveguide (CPW) configurations. The attempts for multiband printed antennas, mainly monopoles, can be summarized in the following techniques: (1) using folded/meandered line as radiators [4, 5]. However, these are mainly dual-band antennas with difficulties in designing more operating bands; (2) using different radiating resonators on top of a radiating patch. This technique is good for dual-band antennas but is difficult to be implemented for triple band and more. Also, it increases the overall monopole size [6, 7]; (3) using different radiating resonators on both top and bottom of a patch [8–10]. The drawback is that the antenna has two functioning faces, which increase the complexity; (4) using different interconnected radiating resonators on top of the patch. This can be understood as cutting slots in the monopole for achieving many operating bands [11, 12]. The cutting shapes should be half wave length to form resonators, which increases the overall antenna size; (5) using slotted monopole on the radiator or ground to excite multiple resonant modes [13–15]. The cutting shapes should be half wave length to form resonators; and (6) using different radiating resonators on three-dimensional (3D) connection [16], which is mainly for mobile handset.

Recently, newly developed artificial meta-materials have been introduced for various microwave devices and components [17–20]. Increasing attention has been paid on by electromagnetic waves community in employing them for novel functionalities and size reduction that cannot be achieved using conventional materials. Left-handed meta-materials (LHMs) are one of these meta-materials, which are characterized by simultaneous negative permittivity and permeability. Realization of LHMs has been proposed in different planar structures, such as transmission line (TL) loaded periodically with series capacitors and shunt inductors, i.e. TL approach. In practice, this approach is constructed of a left handed (LH) TL, which consists of LH elements and parasitic right handed (RH) elements, i.e. a composite right left handed (CRLH) TL [17]. Based on CRLH TL, many novel microwave

[1]Electromagnetic Waves Group, Department of Electronic Engineering, Military Technical College, Cairo, Egypt
[2]Microwave and Communication Systems Group, School of Electrical and Electronic Engineering, University of Manchester, Manchester, UK
Corresponding author:
M.A. Abdalla
Email: maaabdalla@ieee.org

components have been reported, such as resonator [21], balun [22], coupler [23], impedance transformer [24], power splitters [25], phase shifter [26], circulator [27], filters [28–30] to name a few.

The techniques used in planar metamaterial multiband antennas can be summarized, continuing to the aforementioned techniques; as (7) using CRLH TL cells as radiators [31–41], including ultra compact zeroth order antennas [31–36]. These antennas are compact and can be designed to work in arbitrary operating band. However they have very small gain and are difficult in controlling spurious harmonics. Also, they have been employed to load a conventional antennas such as (8) loading dipole antenna [42, 43] and (9) loading monopole antenna [44–46] with CRLH cells. These antennas can have arbitrary operating band, simple in realization and have reasonable gain, but are not very compact. However, in case of loading conventional antennas with a complete CRLH cell, this may increase the overall monopole antenna size and sometimes needs more processing phases in case of implementation since they need the ground for CRLH realization.

Later on, it has been shown that Epsilon negative and Mu negative have an imaginary propagation constant such that they have a band stop resonance properties [47]. These new ideas have contributed as (10) multiband antennas employing negative Mu [48, 49] and negative Epsilon [50, 51]. Finally, (11) using simplified half mode CRLH TL cells as radiator [52, 53]. The antennas can have arbitrary operating band designed and are simple in realization. In [54, 55] loading a monopole antenna with CRLH cells without using a virtual ground plane is presented to introduce dual/triple band antennas. However, no closed analysis procedures were suggested.

In summary, we can conclude that it is very challenging to design multiband antennas, with simple design methodology (arbitrary designed frequencies, arbitrary number of bands), compact in size (does not increase the overall size of the radiator), simple in realization (does not need two layers processing, has good gain (close to typical monopole gain) in addition to low cost. To meet all these challenging requirements, we present the analysis of design producers for simplified multi resonator loaded monopole antenna inspired from half mode CRLH cells introduced as an independent radiator [52] and [53]. As a contribution, a new methodology for loading monopole antenna using two half mode CRLH cells is presented in this paper. The objective of this suggested loading is to introduce simple design procedures and multi band operation in a small antenna size with good antenna gain. In this paper, we provide the detailed analysis and design of a meta-material loaded monopole triple band antenna for all possible WiMAX applications, (2.5–2.7 GHZ, e.g. Multichannel Multipoint Distribution Service (MMDS), 3.3–3.8 GHz, e.g. fixed wireless access (FWA), and 5.3–5.9 GHz, e.g. U-NII-1: 5.15–5.25 GHz, U-NII-2: 5.25–5.35 GHz, U-NII-2e: 5.47–5.725 GHz, and U-NII-3: 5.725 to 5.825 GHz).

A) Antenna design

A triple band antenna is designed by loading a monopole patch with two metamaterial resonators. The design started by designing a monopole patch for the mid frequency band covering 3.3–3.8 GHz. Two extra operation bands were introduced later thanks to the design flexibility of the planar nature and the versatility of meta-material structures. This will be achieved through a metamaterial CRLH resonator to cover 2.5–2.7 and 5.3–5.9 GHz bands. Through the whole presented design procedures, the employed substrate is the low-cost FR4 substrate with dielectric constant 4.4, tan $\delta = 0.02$, and thickness = 1.6 mm.

B) Mid band monopole patch

The structure of the monopole patch is shown in Fig. 1(a). The monopole is fed by a 50 Ω CPW TL with center line width = 1.5 mm, gap = 0.25 mm, and length = 15 mm. The patch length is 13.5 mm, this is quarter wavelength at designed middle frequency (3.6 GHz). The patch width is 6.5 mm, which was proved being wide enough for good antenna radiation. The simulated antenna reflection coefficient, shown in Fig. 1(d), indicates that the monopole patch can operate at frequencies from 3 to 4.2 GHz mid frequency band (3.3–3.8 GHz). The surface current distribution at 3.6 GHz is illustrated in Fig. 1(b). It shows that the surface current is weaker in the middle and open end parts of the patch, i.e. the radiation was mainly contributed by the two edges. Thus, one may utilize the rest parts of the patch to generate extra resonances at other frequencies, which will not cause much distortion to the existing one. It is also worth of notice that the edge close to the feed line does not contribute to radiation either because of the opposite current flow as noted from Fig. 1(b).

C) Half mode CRLH cell antenna

In this section, we explain the mechanism of the half mode CRLH cell antenna. The idea of the half mode CRLH cell for antenna applications has been presented in [52, 53]. The equivalent circuits of a lossless CRLH cell are shown in Fig. 2(a). The CRLH cell is formed by loading a TL with series capacitor (C_L) and shunt inductor (L_L) in addition to the TL parasitic capacitor (C_R) and inductor (L_R). By loading the CRLH TL, a compact CRLH antenna can be realized. It has been shown in [56] that the open circuit resonance mode of the zeroth-order mode CRLH antenna is thanks to the shunt branch resonance. On the other hand, the series branch resonance is the corresponding to short circuit loading. The resonance frequencies for the shunt branch (f_{osh}) and the series branches (f_{ose}) can be written as

$$f_{osh} = \frac{1}{2\pi\sqrt{L_L C_R}}, \quad (1)$$

$$f_{ose} = \frac{1}{2\pi\sqrt{L_R C_L}}. \quad (2)$$

It has been shown in [52, 53] that a simpler and ultra compact meta-material antenna is possible by using only open-circuited half mode CRLH cell. In other words, the half mode cell is suggested to be realized using the shunt combination only (C_R and L_L) as shown in Fig. 2(b), where the element L_R corresponding to the parasitic inductance, cannot be avoided in practical realization.

In our work, the design for the proposed antenna will be based on the shunt loading of CRLH in open circuit termination. The design for the employed elements (L_L and C_R)

https://doi.org/10.1017/S1759078716000738 Published online by Cambridge University Press

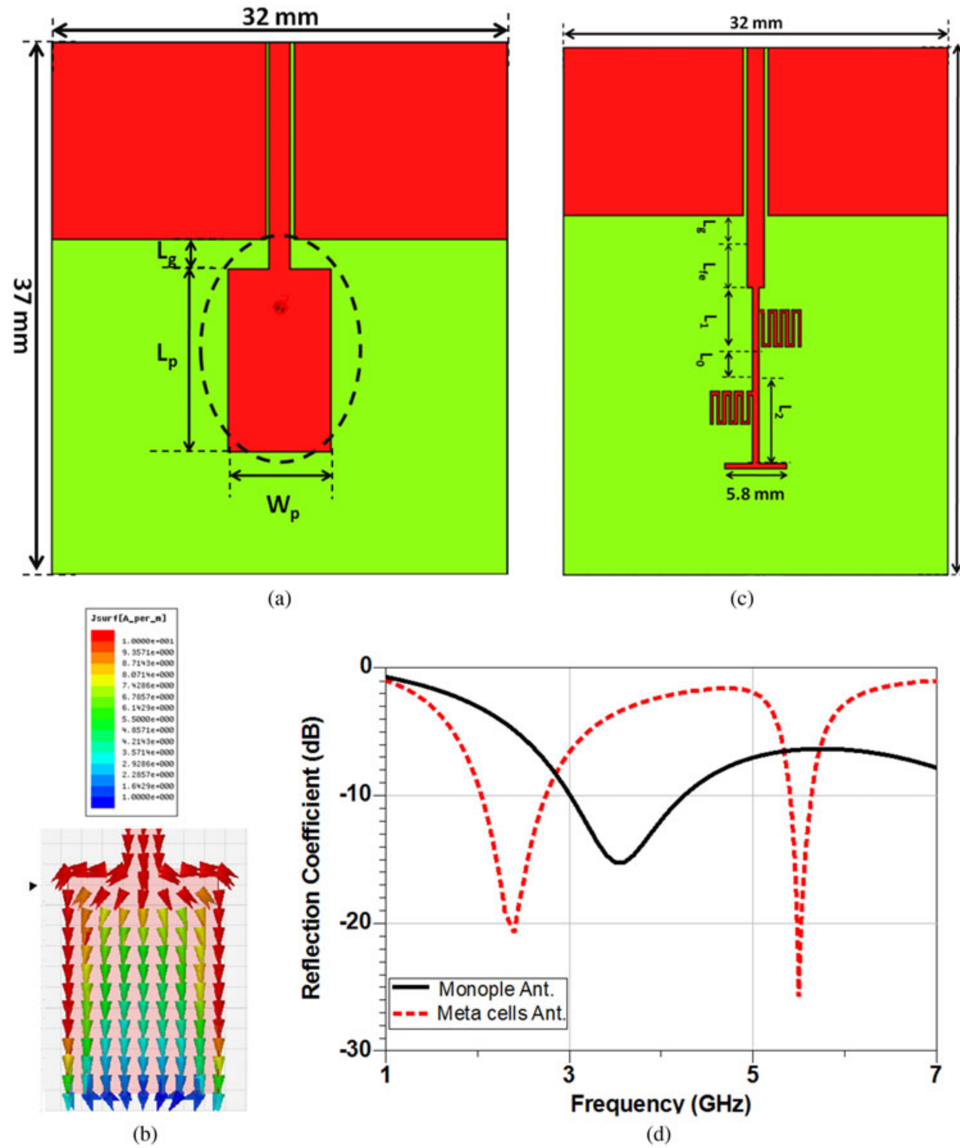

Fig. 1. The mid band monopole antenna to cover 3.3–3.8 GHz band: (a) the layout, (b) the current distributions at 3.6 GHz for 90° phase snapshot, (c) the geometry of the two-cells half mode CRLH TL loaded antenna, where $L_g + L_{fe} = 3$ mm, $L_1 = 6$ mm, $L_2 = 6$ mm, and $L_o = 2$ mm, (d) the simulated reflection coefficient of the monopole patch (black solid line) and meta-material monopole antenna loaded with two-cells half mode CRLH TL (red dash line).

will be extracted by adjusting the desired frequency f_{osh} in (1) to the required frequency.

To illustrate the claimed half mode based antenna operating principle, two different CPW fed configurations for single cell half mode CRLH resonator antennas have been studied to operate at 5.5 and 2.4 GHz as illustrated in Figs 3(a) and 3(b), respectively. In both cases, the half mode CRLH cells are formed by a strip inductor and closed parallel lines capacitor. In Fig. 3(a), the inductor is a strip of length of L_1 whereas in Fig. 3(b), it is formed by T shaped strip. In both cases, the strip inductor is connected to seven closed parallel lines capacitor. The line width and separation are 0.2 mm and length 1.5 mm. It is obvious that the employed elements are connected so that the current will be divided, in shunt configuration, which satisfies the equivalent circuit in Fig. 2(b).

It is worth to comment that the optimization between the cell size and the resonant frequency will limit the design of C_R and L_L to match the monopole size. Accordingly, the dimensions were selected to satisfy (1) at the two design frequencies. The electrical values for half mode CRLH cell elements can be calculated as in [57]. It is worth to comment that the idea of designing these two half mode CRLH cells configuration is to load the patch by their complementary version, the closed parallel lines capacitor will become an interdigital capacitor and strip will become a slot, which will be explained later. Therefore, the suggested configuration yields compact meta-material antenna resonators at different locations on the patch that will be used to achieve lower resonance to cover the 2.5–2.7 GHz band and higher one for 5.3–5.9 GHz band.

The simulated reflection coefficients for the two half mode configurations antennas are shown in Fig. 3. As shown in the figure, the antennas in Figs 3(a) and 3(b), resonates at 5.5 and 2.5 GHz, respectively. The shift in the frequency is due to the higher value of the inductor in Fig. 3(b) as can be predicted from (1). Next the two half mode CRLH -cells antenna is studied, as shown in Fig. 1(c). The structure comprises T shaped strip loaded with two open ended meandered line

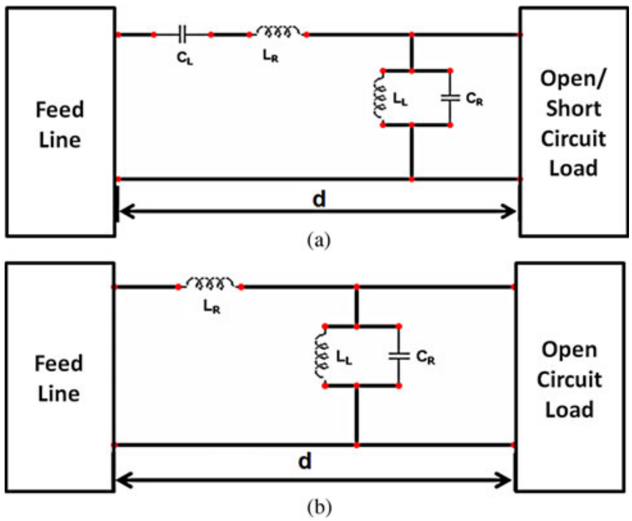

Fig. 2. The equivalent circuit model of the CRLH TL antenna: (a) the full mode case, (b) the practical half mode.

capacitor. The dimensions of the two cell configuration are almost the same as given in Fig. 3 with slight variation for matching enhancement at the operating frequencies. The simulated reflection coefficient of the two half mode CRLH

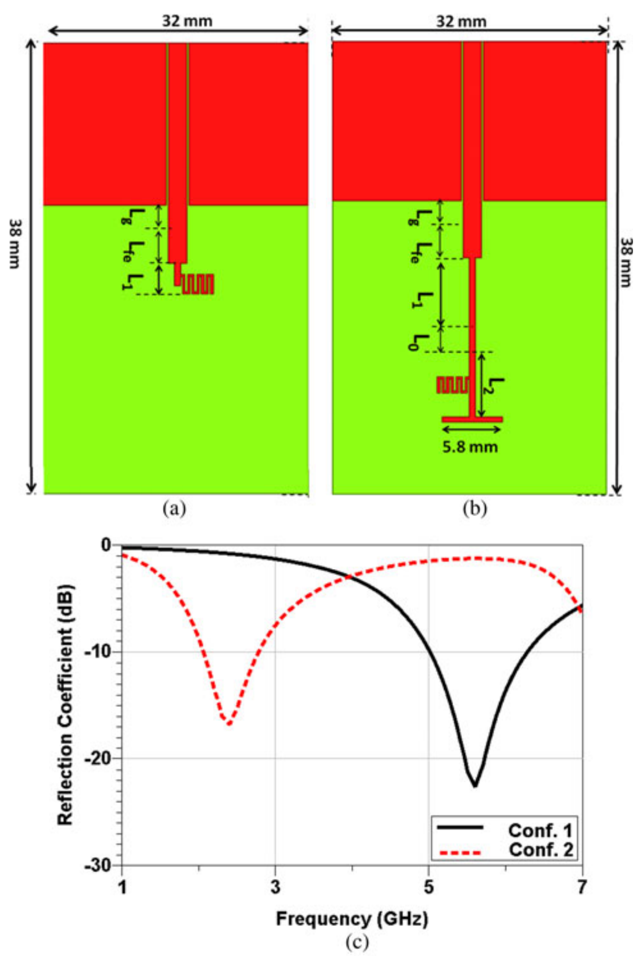

Fig.3. The geometry of the one cell half mode CRLH TL loaded antenna, where $L_g + L_{fe} = 3$ mm: (a) conf. 1, $L_1 = 3$ mm (b) conf. 2, $L_1 + L_2 + L_o =$ 12mm, (c) the simulated reflection coefficients for the single cell half mode CRLH antenna (conf. 1 is (a), conf. 2 is (b)).

cells antenna is shown in Fig. 1(d). It becomes clear that the antenna has better than −10 dB reflection coefficient at two desired bands

D) Integrated monopole and complementary half mode CRLH cell antenna

The triple band antenna is based on the integration of the aforementioned two antennas (the monopole patch and the complimentary half mode CRLH cell antenna). In particular, the meta-material half mode CRLH cell is subtracted from the monopole patch. The resultant antenna layout is shown in Fig. 4. Now, each complementary half mode cell is constructed using an interdigital capacitor and a short slot. The slot is of a T shape so to make the overall antenna compact. Here the interdigital capacitors have four fingers with gaps of 0.2 mm, and finger length of 1.2 mm. Further analysis of the structure, however, reveals that the antenna in Fig. 4(c) does not provide triple band radiation. As it can be seen in Fig. 4, this layout actually has only a single resonance within the spectrum of interests.

To introduce extra resonances, we have shorted the slot at middle because there is a need of extra path for surface current to generate extra resonances. The modified antenna layout is shown in Fig. 5 where the two complementary half mode CRLH cells are separated with distance L_o. This allows controlling the resonant frequency for each cell independently. The electromagnetic full wave simulation results of the modified antenna are shown in Fig. 5(c). It is clear that the antenna, except for the case $L_o = 0$, demonstrates triple band behaviors

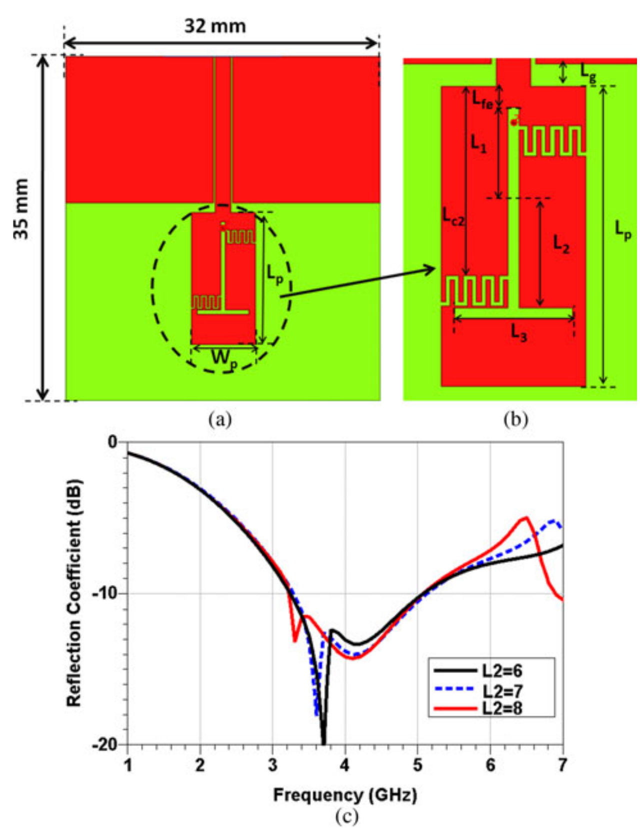

Fig. 4. (a) The layout of the integrated monopole patch with half mode CRLH cells, (b) the simulated reflection coefficients of the integrated monopole antenna with half-mode CRLH TL cells for different slot lengths.

https://doi.org/10.1017/S1759078716000738 Published online by Cambridge University Press

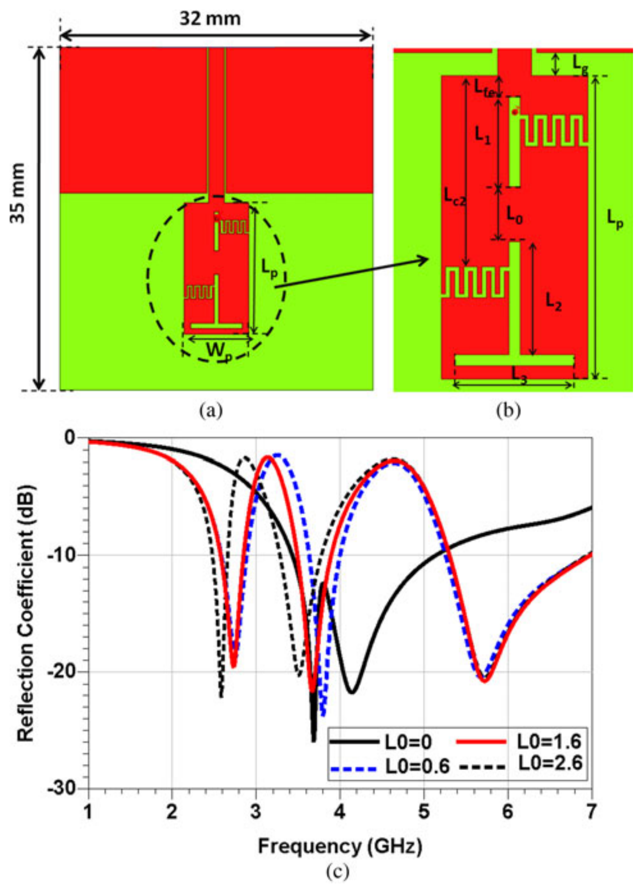

Fig. 5. (a) The layout of the triple band meta-material half mode CRLH loaded monopole antenna, (b) the simulated reflection coefficients of the meta-material half mode CRLH TL loaded triple band antenna for different length of L_o.

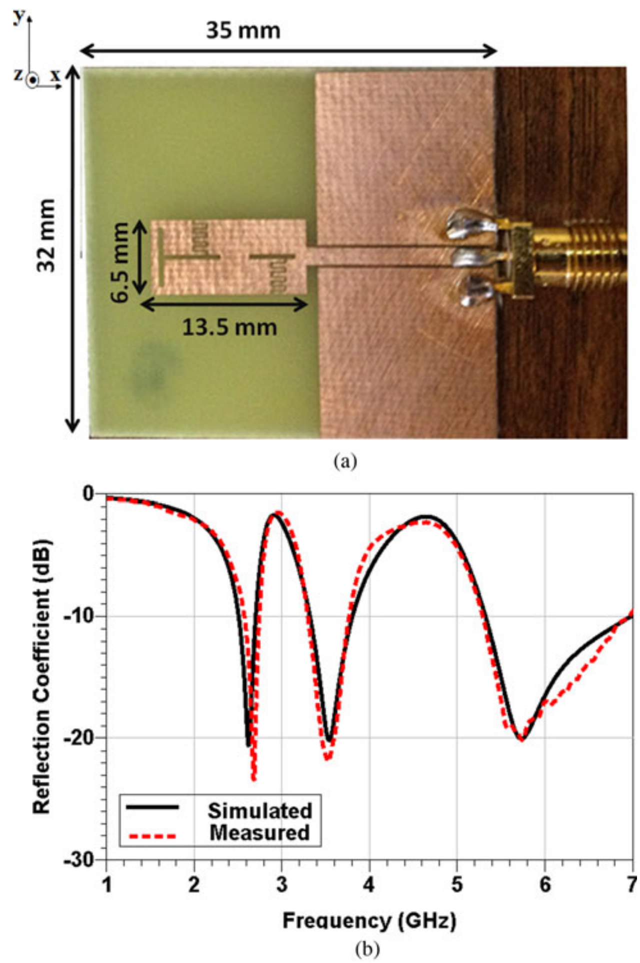

Fig. 7. A photograph of the fabricated triple band meta-material half-mode CRLH cell loaded monopole antenna, (b) simulated and measured reflection coefficients of the triple band meta-material half-mode CRLH cell loaded monopole.

centered approximately around 2.6, 3.6, and 5.8 GHz, respectively with relatively small effects of non-zero L_o.

To better understand the mechanism for inducing extra resonances, the surface current distribution is illustrated in Fig. 6. It becomes clear that the two half mode CRLH cells loading have forced the majority surface current in phase along the monopole in the x-axis at the resonant frequencies so to enable the monopole mode radiations.

E) Antenna measurements

The fabricated triple band meta-material half mode CRLH TL loaded antenna is shown in Fig. 7(a). To illustrate the antenna design compactness, we have compared the final designed radiator patch (13.5×6.5 mm²) to conventional

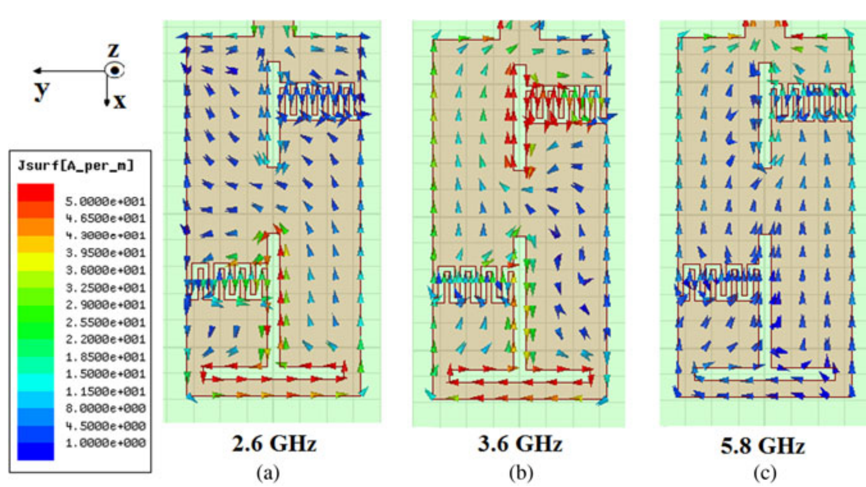

Fig. 6. The current distribution of the triple band meta-material half mode CRLH loaded antenna at (a) 2.6 GHz, (b) 3.6 GHz, and (c) 5.8 GHz.

https://doi.org/10.1017/S1759078716000738 Published online by Cambridge University Press

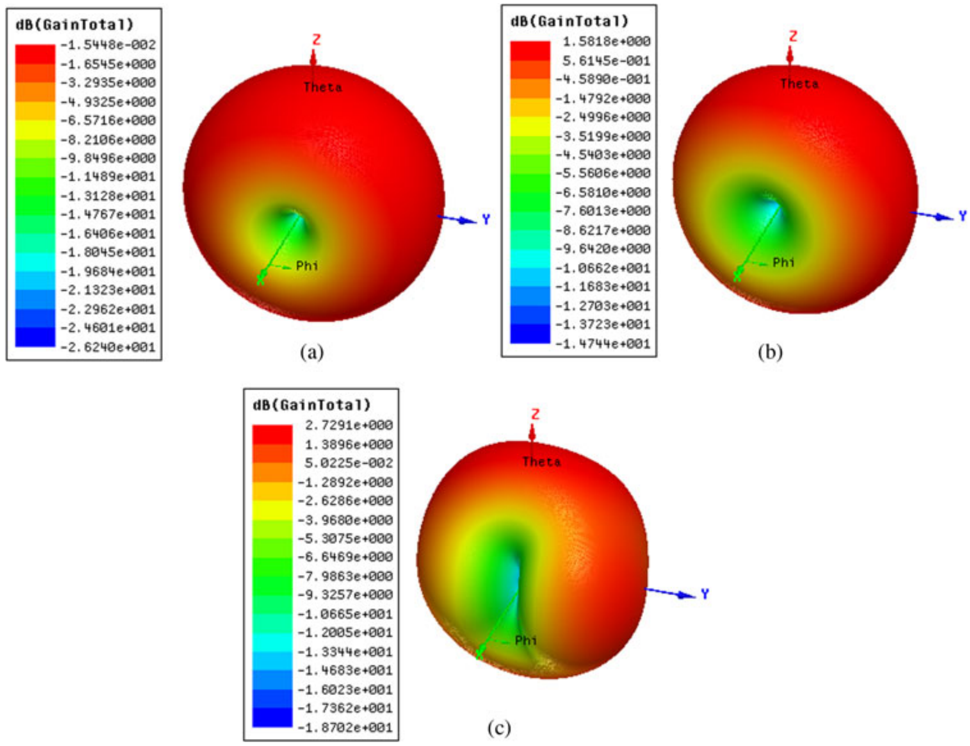

Fig. 8. The 3D radiation pattern: (a) at 2.6 GHz, (b) at 3.6 GHz, (c) at 5.8 GHz.

single band microstrip patch antenna. For the same feeding TL length (20 mm), the single patch size is 36.5×28.5 mm^2 at 2.5 GHz, with overall antenna of 80×64 mm^2, with overall antenna size $= 62 \times 49$ mm^2, at 3.5 GHz and 16.6×14.4 mm^2 at 5.5 GHz, with overall antenna size $= 46 \times 34$ mm^2. From this comparison, we can claim that the novel triple band radiator size has been reduced by 91% and the whole antenna by 75% at 2.5 GHz, 83 and 48% at 3.5 GHz and 47 and 18% at 5.5 GHz.

The electromagnetic full wave simulation and measured reflection coefficients of the triple band meta-material antenna are given in Fig. 7(b). The measured first operating band is centered at 2.6 GHz with -10 dB bandwidth extending from 2.5 to 2.7 GHz. Similarly, the second operating band is centered at 3.6 GHz and extends from 3.3 to 3.8 GHz. The third band is centered at 5.8 GHz and extends from 5.3 GHz to almost 7 GHz. The figure illustrates very good agreement between the measured and the simulated results, demonstrating that the novel meta-material monopole antenna suits very well for multiband WiMAX applications. These results validate the antenna aforementioned design procedures.

The antenna radiation performance at the three operating bands has also been investigated by examining the radiation patterns at center frequencies of the operating bands both numerically and experimentally. The 3D simulated radiation pattern at 2.6 GHz is depicted in Fig. 8(a), clearly showing a typical omnidirectional pattern (doughnut-like). The simulated gain is about 0 dBi and radiation efficiency 0.868. The simulated and measured co- and cross-polarization radiation patterns in the *E*-plane (*XZ*-plane, $\phi = 0°$) and *H*-plane (*YZ*-plane, $\phi = 90°$) are depicted in Figs 9(a) and 9(b), respectively. As it can be seen, the simulated (solid black line) and measured (dash red line) co-polarizations in *E*-plane show good agreement. Both demonstrate typical eight-like shape radiation patterns due to *x*-direction linear electric field polarization. This is consistent with the surface current along the *x*-axis in Fig. 9(a). The measured gain is about 0.7 dBi, polarizations are apart. The cross-polarization was mainly caused by slightly higher than the simulated one of 0 dBi. On the other hand, the simulated (solid purple line) and measured (dash green line) cross- *y*-directed current induced by the half mode CRLH cell close to the open end of the patch as shown in Fig. 6(a), resulting relatively higher cross-polarization in the $-x$-direction, i.e. in the right-half of Fig. 9(a). The much larger measured cross-polarization is likely caused by the interference of unbalanced current occurring on the two CPW ground planes due to the lack of air-bridge connecting them.

In the *H*-plane, both simulated and measured co-polarization patterns are omnidirectional and agree very well. The 3D simulated radiation pattern at 3.6 GHz is plotted in Fig. 8(b). As we can observe the antenna preserves the typical omnidirectional shape and it is close to that pattern at first operating band (2.6 GHz) shown earlier in Fig. 8(a). As shown, the simulated gain is 1.58 dBi. The simulated radiation efficiency is 0.895. The simulated and measured co- and cross-polarizations in *E*-plane (*XZ*-plane, $\phi = 0°$) and *H*-plane (*YZ*-plane, $\phi = 90°$) are shown in Figs 9(c) and 9(d), respectively. The simulated and measured co-polarization radiation patterns are largely in good agreement. The discrepancies mainly in the $+x$-direction, i.e. in the left-half of Fig. 9(c), probably again caused by the un-balanced CPW ground planes. It is interesting to see that the cross-polarized *E*-field has a dipole mode. This is attributed from the stronger in-phase surface currents along the edge of the monopole close to the CPW feed line than the opposite surface current along the edge of the open end, as shown in Fig. 6(b), which results in higher cross-polarization in the +

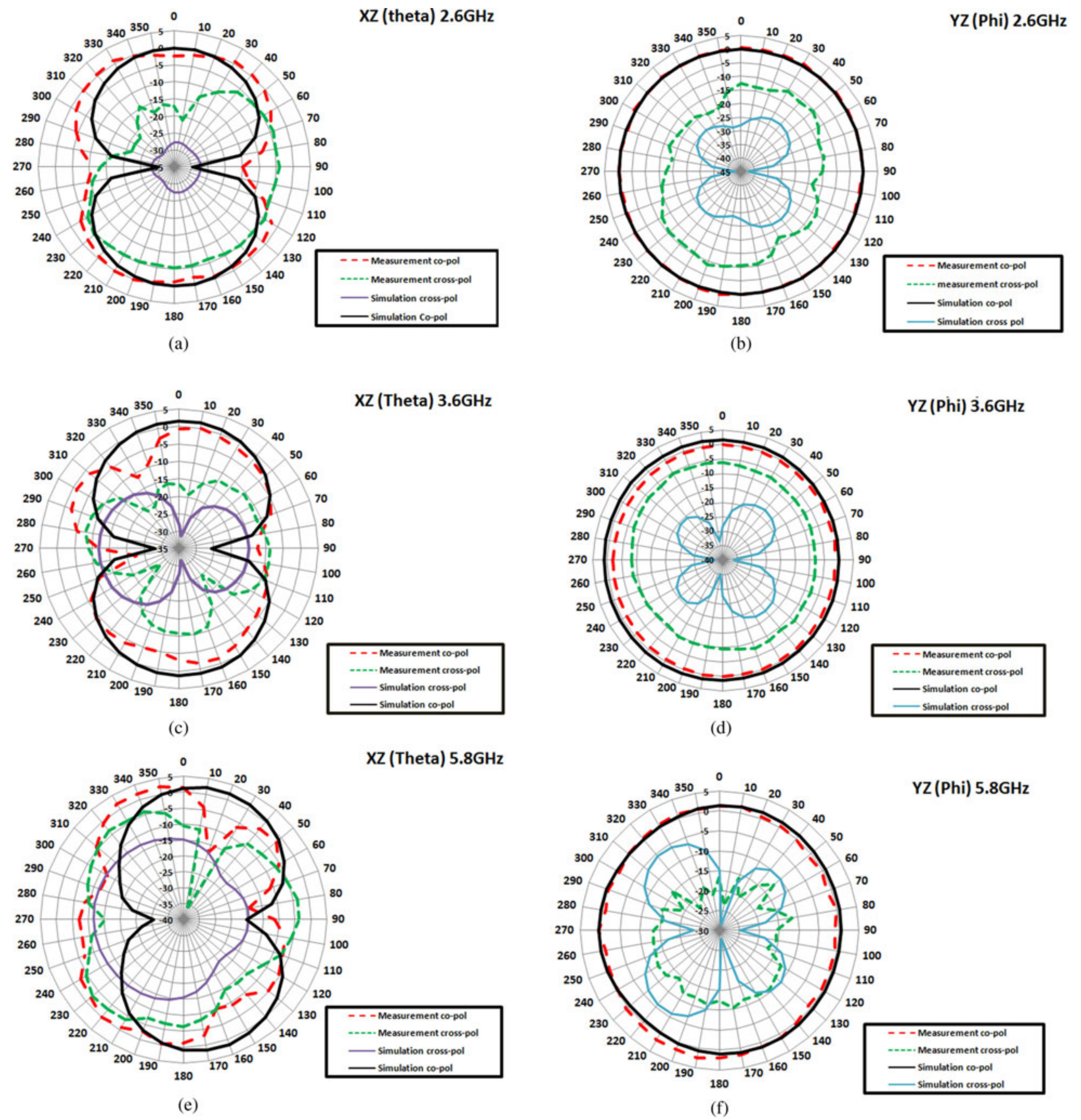

Fig. 9. Comparison between the simulated and measured co- and cross-polarization radiation patterns (a), (b) at 2.6 GHz in: (a) *E*-plane (*XZ*-plane, $\phi = 0^o$) and (b) *H*-plane (*YZ*-plane, $\phi = 90^o$); (c), (d) at 3.6 GHz in (c) *E*-plane (*XZ*-plane, $\phi = 0^o$) and (d) *H*-plane (*YZ*-plane, $\phi = 90^o$); (d), (e), (f) at 5.8 GHz in (e) *E*-plane (*XZ*-plane, $\phi = 0^o$) and (f) *H*-plane (*YZ*-plane, $\phi = 90^o$).

x-direction. In the *H*-plane, the simulated and measured co-polarized *H*-field patterns are in good agreement. The measured gain at 3.6 GHz is 0 dBi, lower than the simulated one of 1.6 dBi.

At 5.8 GHz, the 3D simulated gain pattern is plotted in Fig. 8(c). It can be observed at higher frequency band the radiation pattern become less doughnut-like on $+x$-direction. The cause of this can be observed from Fig. 10, showing the two CPW ground planes also radiate. However, the x-directed surface current on the two CPW ground planes is opposite to the x-directed surface current on the patch, resulting in less gain on the $+x$-direction. This can also be clearly seen in Fig. 9(e). The simulated gain is 2.729 dB and radiation efficiency is 0.905. In Fig. 9(f), it can be seen that the simulated and measured co-polarized *H*-fields are in good agreement. The measured gain is 1.6 dBi, lower that the simulated one of 2.73 dBi.

Based on the previous results, we can claim that the small discrepancies between measured and simulated results were mainly due to the effect of the non-avoided reflections during measurements such as the reflection from the SMA connector whose size is comparable with the radiator size.

Also, it is worth to explain that the measured gain procedure was done based on the three antenna method. This method was used based on the single antenna under test in addition to two different antennas (operating at the same

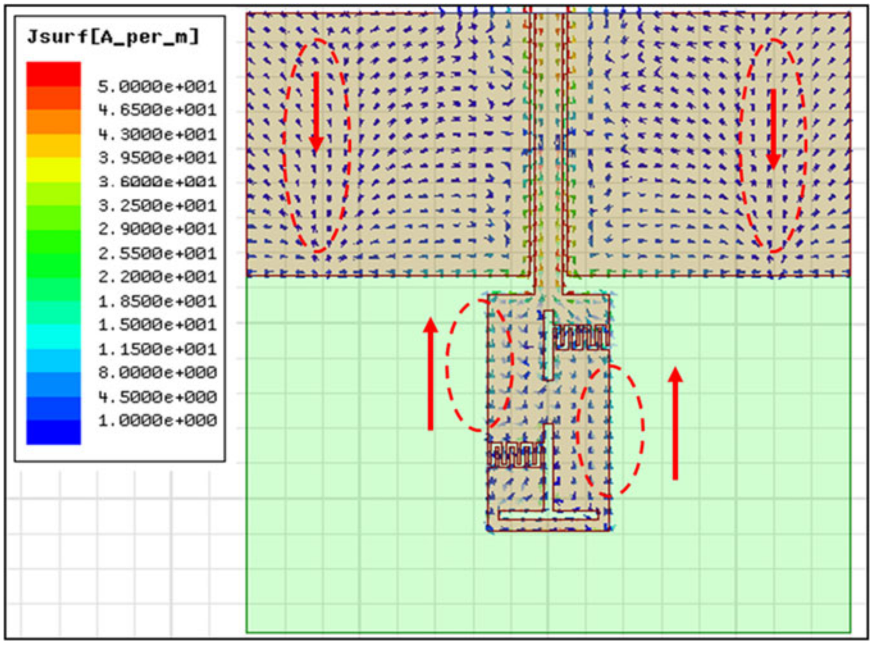

Fig. 10. The surface current distribution at 5.8 GHz.

Table 1. A comparison between introduced antenna in this paper and recent previous work.

Parameter	Method	Band # 1	Band # 2	Band # 3
Center frequency (GHz)	Simulated	2.62	3.55.	5.75
	Measured	2.63	3.55	5.75
Return loss at center frequency (dB)	Simulated	21	20	20
	Measured	23	22	20
10 dB return loss at center frequency (MHz)	Simulated	200	250	1600
	Measured	200	250	1600
Gain (dB)	Simulated	0	1.6	2.73
	Measured	0.7	0	1.6

Table 2. A comparison between triple band antennas (recent published and the proposed antenna in this paper).

Reference	Frequency band (MHz)	−10 dB fractional bandwidth (%)	Substrate dielectric constant (ε_r)	Average antenna gain (dBi)	Physical substrate size (length × width × height (mm³))	Electrical antenna largest dimension (in terms of free space wavelength) at mid frequency (%)
This work	2.5–2.7	7.7	4.4	0	35 × 32 × 1.6	30.4
	3.3–3.8	14.1		1.6		41.4
	5.3–5.9	10.7		2.7		65.2
[4]	2.36–2.57	8.4	4.4	−2	15 × 40 × 0.8	32.9
	3.05–3.62	17.62		−2.1		44.4
	5.26–5.86	10.81		−1.2		70.1
[9]	2.14–2.52	16.3	4.4	2.4	30 × 20 ×1.6	23.3
	2.82–3.74	28		2.35		32.8
	5.15–6.02	15.6		2.95		55.8
[11]	2.35–2.58	9.33	4.4	−0.3	40 × 40 × 0.8	33.05
	3.25–4	20.7		0.9		48.36
	4.95–5.9	17.5		3.6		72.5
[14]	2.25–2.85	23.5	4.4	2.3	15 × 15 × 1.6	12.7
	3.4–4.15	3.775		2.8		21.2
	4.45–8	6.225		3.15		31.2
[39]	1.74–1.81	3.08	2.2	−0.15	20 × 20 × 0.508	11.8
	4.2–5	15.17		2.2		30.8
	5.7–6.6	8.33		3.5		41
[45]	0.9–0.93	3.27	2.33	2.8	95 × 56 × 1.57	29.05
	1.22–1.23	0.8		3.1		38.9
	1.65–2.6	44.7		3.2		67.5

bandwidth). The method is based on measuring the received power from transmitting one using each pair of the three antennas, which is calculated as

$$G_{idB} + G_{jdB} = 20\log\left(\frac{4\pi R}{\lambda}\right) + 10\log\left(\frac{P_r}{P_t}\right)^{(k)}, \qquad (3)$$

where i and j referes to the two different antennas (antenna # i and antenna # j) measured during experiment #k ($k = 1, 2,3$). The measurement was done at a fixed distance (enough to satisfy the far field criterion) between transmitting and receiving antennas. Thus, this method allows the calculation of the three antenna gains. More details about the method can be found in [58].

In summary, the performance of the proposed triple band antenna is tabulated in Table 1.

Finally, a comparison between the proposed antenna and recent triple band compact size antenna are summarized in Table 2. The comparison demonstrates competitive features for the proposed antenna in terms of its compact size, good gain. Also, it is worth to comment that the proposed antenna has suitable bandwidth for wireless services, which is neither too large to suffer interference nor too narrow to affect the service.

II. CONCLUSION

The technique for designing multiband antennas based on loading the monopole antenna with simplified half mode CRLH cells has been proposed. A case study for triple band antenna has been experimentally demonstrated. The antenna has been designed to cover three bands (2.5–2.7 band, 3.3–3.8 band, and 5.3–5.9 GHz band) based on the proposed technique. The monopole patch itself introduces middle resonance whereas the two-cell CRLH TL loading provides extra two resonances at lower and upper frequency bands. The fabricated antenna has a size of 35 × 32 mm. The antenna's radiation patterns further validate the design both numerically and experimentally, showing that simulated and measured E- and H-fields are largely in a good agreement. Good radiation efficiency and antenna gain have been achieved at all three bands.

REFERENCES

[1] Chen, X.: Ultra-wideband antennas and propagation for communications, radar and imaging, WILEY, 2007.

[2] Wong, K.: Compact and Broadband Microstrip Antennas, John Wiley & Sons, Inc., New York, 2002.

[3] Weiner, M.M.: Monopole Antennas, Marcel Dekker Int, New York, NY, 2003.

[4] Park, Y.K.; Kang, D.; Sung, Y.: Compact folded triband monopole antenna for USB dongle applications. IEEE Antennas Wireless Propag. Lett., **11** (2012), 228–231.

[5] Sim, D.; Moon, J.; Park, S.: A wideband monopole antenna for PCS/IMT-2000/Bluetooth applications. IEEE Antennas Wireless Propag. Lett., **3** (1) (2004), 45–47.

[6] Deng, C.; Liu, X.L.; Zhang, Z.; Tentzeris, M.M.: A miniascape-like triple-band monopole antenna for WBAN applications. IEEE Antennas Wireless Propag. Lett., **11** (2012), 1330–1333.

[7] Yoon, J.H.; Rhee, Y.C.: A modified three-circular-ring monopole antenna for WLAN/WiMAX triple-band operations 2013, Asia-Pacific Microwave Conf. Proc. (APMC), 2013, 1142–1144.

[8] Huang, H.; Zhang, S.: A compact triple-band monopole antenna for WLAN/WIMAX application, 2013 Proc. of the Int. Symp. on Antennas & Propagation (ISAP), vol. **01**, 2013, 454–457.

[9] Liu, W.; Wu, C.; Dai, Y.: Design of triple-frequency microstrip-fed monopole antenna using defected ground structure. IEEE Trans. Antennas Propag., **59** (7) (2011), 2457–2463.

[10] Chang, T.-H.; Kiang, J.-F.: Compact multi-band H-shaped slot antenna. IEEE Trans Antennas Propag., **61** (8) (2013), 4345–4349.

[11] Sun, X.L.; Zhang, J.; Cheung, S.W.; Yuk, T.I.: A triple-band monopole antenna for WLAN and WiMAX applications. 2012 IEEE Antennas and Propagation Society Int. Symp. (APSURSI), USA, 2012, 1–2.

[12] Moeikham, P., Mahatthanajatuphat, C., Akkaraekthalin, P.: A triple band printed monopole antenna for WLAN/WiMAX applications, 2012 Int. Symp. on Antennas and Propagation (ISAP), Japan, 2012, 295–298.

[13] Mehdipour, A.; Sebak, A.; Trueman, C.W.; Denidni, T.A.: Compact multiband planar antenna for 2.4/3.5/5.2/5.8-GHz wireless applications. IEEE Antennas Wireless Propag. Lett., **11** (2012), 144–147.

[14] Moosazadeh, M.; Kharkovsky, S.: Compact and small planar monopole antenna with symmetrical L- and U-shaped slots for WLAN/WiMAX applications. IEEE Antennas Wireless Propag. Lett., **13** (2014), 388–391.

[15] Chen, C.; Sim, C.; Chen, F.: A novel compact quad-band narrow strip-loaded printed monopole antenna. IEEE Antennas Wireless Propag. Lett., **8** (2009), 974–976.

[16] Niroo-Jazi, M.; Denidni, T.A.: A new triple-band circular ring patch antenna with monopole-like radiation pattern using a hybrid technique. IEEE Trans. Antennas Propag., **59** (10), (2011), 3512–3517.

[17] Caloz, C.; Itoh, T.: Electromagnetic Metamaterials Transmission Line Theory and Microwave Applications, John Wiey & Sons, New Jersey, 2006.

[18] Eleftheriades, G.V.; Balmain, K.G.: Negative Refractive Metamaterials, John Wiey & Sons, New Jersey, 2005.

[19] Marqués, R.; Martín, F.; Sorolla, M.: Metamaterials with Negative Parameters Theory, Design and Microwave Applications, John Wiey & Sons, New Jersey, 2008.

[20] Capolino, F.: Theory and Phenomena of Metamaterials, CRC Press, Boca Raton, FL, 2009.

[21] Karimian, S.; Hu, Z.; Abdalla, M.A.: Compact half-wavelength metamaterial stepped impedance resonator (SIR), in Digest IEEE AP-S Int. Antennas and Propogation Symp., USA, 2011, 2951–2953.

[22] Jung, Y.K.; Lee, B.: Design of compact and wideband metamaterial balun based on closed form solutions. Microw. Opt. Technol. Lett., **52** (2010), 1153–1156.

[23] Taravati, S.; Khalaj-Amirhosseini, M.: Compact dual-band stubless branch-line coupler. J. Electromagn. Waves Appl., **26** (10) (2012), 1323–1331.

[24] Abdalla, M.A.; Wahba, W.; Elregaily, H.; Allam, A.A.; Abdel Nazir, A.: A compact and wideband SIW metamaterial impedance transformer, 2nd MeCAP, Cairo, Egypt, 2012, 1–4.

[25] Abdalla, M.A.; Hu, Z.: Compact and broadband left handed CPW power divider/combiner for C/X bands, 29th National Radio Science Conf. (NRSC2011), Cairo, Egypt, April 10–12, 2012, 29–36.

[26] Abdalla, M.A.; Hu, Z.: Ferrite tunable metamaterial phase shifter, 2010 IEEE AP-S Int. Antenna and Propagation Symp. Digest, Toronto, Canada, July 11–17, 2010, 1–4.

[27] Abdalla, M.A.; Hu, Z.: Compact novel CPW ferrite coupled line circulator with left-handed power divider/combiner, in Digest European Microwave Week, EuMW2011, UK, 2011, 794–707.

[28] Luo, S.; Zhu, L.; Sun, S.: A dual-band ring-resonator bandpass filter based on two pairs of degenerate modes. IEEE Trans. Microw. Theory Tech., **58** (2010), 3427–3432.

[29] Karimian, S.; Hu, Z.: Miniaturized composite right/left-handed stepped-impedance resonator bandpass filter. IEEE Microw. Wireless Compon. Lett., **22** (8) (2012), 400–402.

[30] Abdalla, M.; Hassan, A.Y.; Galal Eldin, A.M.: A compact high selective coupled gap CRLH TL based bandpass filter, 2015 9th Int. Congress on Advanced Electromagnetic Material in Microwave and Optics, UK, 7–12 September 2015, 352–354.

[31] Erentok, A.; Ziolkowski, R.W.: Metamaterial-inspired efficient electrically small antennas. IEEE Trans. Antennas Propag., **56** (3) (2008), 691–707.

[32] Pyo, S.; Han, S.M.; Baik, J.W.; Kim, Y.S.: A slot-loaded composite right/left-handed transmission line for a zeroth-order resonant antenna with improved efficiency. IEEE Trans. Microw. Theory Tech., **57** (11) (2009), 2775–2782.

[33] Kim, T.G.; Lee, B.: Metamaterial-based compact zeroth-order resonant antenna. Electron. Lett., **45** (1) (2009), 12–13.

[34] Abdalla, M.; Hu, Z.; Compact and tunable metamaterial antenna for multi-band wireless communication applications, 2011 IEEE AP-S Int. Antenna and Propagation Symp. Digest, Spokane, USA, 2011, 2951–2953.

[35] Abdalla, M.: A dual mode CRLH TL metamaterial antenna, 2014 IEEE AP-S Int. Antenna and Propagation Symp. Digest, Memphis, USA, 2014, 793–794.

[36] Abdalla, M.A.; Ibrahim, A.A.: Compact and closely spaced metamaterial MIMO antenna with high isolation for wireless applications. IEEE Wireless Propag. Lett., **12** (2013), 1452–1455.

[37] Dong, Y.; Itoh, T.: Miniaturized substrate integrated waveguide slot antennas based on negative order resonance. IEEE Trans. Antennas Propag., **58** (12) (2010), 3856–3864.

[38] Ibrahim, W.; Abdalla, M.; Allam, A.; Mohamed, A.; Elregeily, H.: A compact and dual band metamaterial substrate integrated waveguide antenna, 2013 IEEE AP-S Int. Antenna and Propagation Symp. Digest, Orlando, USA, June 7–13, 2013, 966–967.

[39] Amani, N.; Kamyab, M.; Jafargholi, A.; Hosseinbeig, A.; Meiguni, J.S.: Compact tri-band metamaterial-inspired antenna based on CRLH resonant structures. Electron. Lett., **50** (12) (2014), 847–848.

[40] Pham, B.L.: Triple bands antenna and high efficiency rectifier design for RF energy harvesting at 900, 1900 and 2400 MHz, 2013 IEEE MTT-S Int. Microwave Symp. Digest (IMS), 2013, 1–3.

[41] Abdalla, M.; Sadek, F.H.: Compact triple-band left-handed antenna For GSM/WiMAX applications, 2015 9th Int. Congress on Advanced Electromagnetic Material in Microwave and Optics, UK, September 2015, 295–297.

[42] Saurav, K.; Sarkar, D.; Srivastava, K.V.: CRLH unit-cell loaded multi-band printed dipole antenna. IEEE Antennas Wireless Propag. Lett., **13** (2014), 852–855.

[43] Abdalla, M.; El-Dahab, M.; Ghouz, M.: Dual/Triple band printed dipole antenna loaded with CRLH cells, 2014 IEEE AP-S Int. Antenna and Propagation Symp. Digest, Memphis, USA, 2014, 1007–1008.

[44] Ibrahim, A.A.; Safwat, A.M.E.; El-Hennawy, H.: Triple-band microstrip-fed monopole antenna loaded with CRLH unit cell. IEEE Antennas Wireless Propag. Lett., **10** (2011), 1547–1550.

[45] Ibrahim, A.A.; Safwat, A.M.E.: Microstrip-fed monopole antennas loaded with CRLH unit cells. IEEE Trans. Antennas Propag., **60** (9) (2012), 4027–4036.

[46] Bala, B.D.; Rahim, M.K.A.; Murad, N.A.: A compact triple mode metamaterial inspired-monopole antenna for wideband applications, 2013 Proceedings of the Int. Symp. on Antennas & Propagation (ISAP), vol. **2**, 2013, 1127–1130.

[47] Alù, A.; Engheta, N.: Pairing an epsilon-negative slab with a mu-negative slab: resonance, tunneling and transparency. IEEE Trans. Antennas Propag., **51** (10) (2003), 2558–2571.

[48] Abdalla, M.; Ibrahim, A.: Design of close, compact, and high isolation meta-material MIMO antennas, 2013 IEEE AP-S Int. Antenna and Propagation Symp. Digest, Orlando, USA, 2013, 186–187.

[49] Wei, K. et al.: A wideband MNG-TL dipole antenna with stable radiation patterns. IEEE Trans. Antennas Propag., **61** (5) (2013), 2418–2424.

[50] Niu, B.; Feng, Q.; Shu, P.: Epsilon negative zeroth-and first-order resonant antennas with extended bandwidth and high efficiency. IEEE Trans. Antennas Propag., **61** (12) (2013), 5878–5884.

[51] Huang, J.Q.; Chu, Q.X.: Compact epsilon negative zeroth order resonator antenna with higher radiation efficiency. Microw. Opt. Technol. Lett., **53** (4) (2011), 897–900.

[52] Abdalla, M.A.; Hu, Z.: A compact dual band meta-material antenna for wireless applications, 2012 Loughborough Antennas & Propagation Conf., Loughborough, UK, 2012, 1–4.

[53] Abdalla, M.; Fouad, M.; Ahmed, A.; Hu, Z.: A new compact microstrip triple band antenna using half mode CRLH transmission line, 2013 IEEE AP-S Int. Antenna and Propagation Symp. Digest, Orlando, USA, 2013, 634–635.

[54] Zhu, J.; Eleftheriades, G.V.: Dual-band metamaterial-inspired small monopole antenna for WiFi applications. Electron. Lett., **45** (22) (2009), 1104–1106.

[55] Abdalla, M.A.; Abdelnaby, U.; Mitkees, A.A.: Compact and triple band meta-material antenna for All WiMAX applications, 2012 Int. Symp. on Antennas and Propagation (ISAP), 2012, 1176–1179.

[56] Rennings, A.; Liebig, T.; Caloz, C.; Waldow, P.: MIM CRLH Series Mode Zeroth Order Resonant Antenna (ZORA) implemented in LTCC Technology, APMC 2007. Asia-Pacific Microwave Conf., 2007, 1–4.

[57] Hong, J.: Microstrip Filters for RF/Microwave Application, Wiles and Sons, New Jersey, 2011.

[58] Balanis, C.A.: Antenna Theory: Analysis and Design, 3rd ed, John Wiley & Sons, Hoboken, 2012, 867–868.

Mahmoud Abdelrahman Abdalla was born in 1973, received the B.Sc. degree, with grade of excellent with honors, in Electrical Engineering from the Electronic Engineering Department, Military Technical College, Cairo, Egypt in 1995. He was awarded the M.Sc. degree in Electrical Engineering from Military Technical College in 2000, and the Ph.D. degree from Microwave and Communication group, School of Electrical Engineering, Manchester University, UK, in 2009.

He has been with Military Technical College since 1996 where he is now an Associate Professor in Electronic Engineering Department. His research has focused on different metamaterial applications in microwave and millimeter bands specially microwave components, miniaturized multiband antennas, and ferrite components. Also his research includes electromagnetic energy harvesting systems, EBG components, adaptive antenna systems for DOA estimation and interference cancellations, and radar absorber designs. He has published about 100 peer-reviewed journal and conference papers. Dr. Mahmoud Abdalla is a senior member of the IEEE and the European Microwave Association EuMA. He is currently a reviewer in many electromagnetic journals such as IEEE Antennas and Wireless Propagation Letters, IEEE transaction in Magnetics, IET Microwave, antenna and propagation, International Journal of Microwave and Wireless Technologies, Journal of electromagnetic waves (JEMW), Progress in Electromagnetic Research, European Physical Journal – Applied Physics, Journal of Applied Computational Electromagnetic Society, Advanced Electromagnetic and some others.

Zhirun Hu (M'98) received his B.Eng in Communication Engineering from Nanjing, China, in 1982, Master in Business Administration, and Ph.D. in Electrical and Electronic engineering from the Queen's University of Belfast, United Kingdom, in 1988 and 1991, respectively.

In 1991, he joined the Department of Electrical and Electronic Engineering, University College of Swansea, as a senior research assistant in computational semiconductor device simulation. In 1994, he was with the Department of Electrical and Electronic Engineering, the Queen's University of Belfast, as a research fellow in silicon MMIC design, realization and characterization. In 1996, he joined GEC Marconi, as a microwave technologist working on microwave/millimetre-wave device and circuit design and characterization. He was a lecturer with the Department of Electronic Engineering, King's College London from 1998 to 2003. He is now with the School of Electrical and Electronic Engineering, the University of Manchester. He has published more than 200 peer-reviewed journal and conference papers.

Cahyo Muvianto received all degree in Electrical and Electronic Engineering, Bachelor from the ITS, Surabaya, Indonesia, in 1995, M.Sc. degree From University of Manchester Institute of Science and Technology (UMIST), and Ph.D. degree from The University of Manchester, Manchester – UK, in 2001 and 2012, respectively. From 1995 to 2000, he worked at radio paging company as chief of engineer and later as operation manager in Mataram-Indonesia. He joined the Department of Electrical Engineering, University of Mataram- Indonesia as lecturer in 1998. He is currently as Research Associate with the School of Electrical and Electrical Engineering, The Manchester University. His research work is focused on microwave sensors and applications systems.

https://doi.org/10.1017/S1759078716000738 Published online by Cambridge University Press